Accepted Manuscript

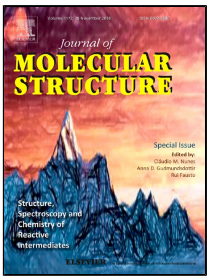

Influence of proline and β-Cyclodextrin in ketoconazole physicochemical and microbiological performance

Ariana Zoppi, Natalia Buhlman, Juan Pablo Cerutti, Marcela R. Longhi, Virginia Aiassa

PII:	S0022-2860(18)31043-3
DOI:	10.1016/j.molstruc.2018.08.094
Reference:	MOLSTR 25615
To appear in:	*Journal of Molecular Structure*
Received Date:	18 May 2018
Accepted Date:	28 August 2018

Please cite this article as: Ariana Zoppi, Natalia Buhlman, Juan Pablo Cerutti, Marcela R. Longhi, Virginia Aiassa, Influence of proline and β-Cyclodextrin in ketoconazole physicochemical and microbiological performance, *Journal of Molecular Structure* (2018), doi: 10.1016/j.molstruc.2018.08.094

INFLUENCE OF PROLINE AND β-CYCLODEXTRIN IN KETOCONAZOLE PHYSICOCHEMICAL AND MICROBIOLOGICAL PERFORMANCE

Ariana Zoppi [a, b], Natalia Buhlman[a], Juan Pablo Cerutti[a], Marcela R. Longhi [a, b], Virginia Aiassa [a, b]*.

[a] Departamento de Ciencias Farmacéuticas, Facultad de Ciencias Químicas, Universidad Nacional de Córdoba, Córdoba, Argentina. Tel. +549 0351 5353865 int. 53355.

[b] Unidad de Investigación y Desarrollo en Tecnología Farmacéutica (UNITEFA), CONICET, Universidad Nacional de Córdoba, Córdoba, Argentina.

ariana@fcq.unc.edu.ar, natybuhlman@hotmail.com, juampi_94_cerutti@hotmail.com, mrlcor@fcq,unc.edu.ar, aiassa@fcq.unc.edu.ar.

*Corresponding author: Virginia Aiassa. Departamento de Ciencias Farmacéuticas. Facultad de Ciencias Químicas. Universidad Nacional de Córdoba. Haya de la Torre y Medina Allende, s/n. Ciudad Universitaria. X5000HUA Córdoba. Argentina. Tel.: +54-351-5353865 fax: +54-351-5353865. E-mail: aiassa@fcq.unc.edu.ar

Abstract

This investigation presents the characterization and evaluation of the physicochemical and microbiological properties of a new multicomponent complex of ketoconazole. Complex formation of the drug, with proline and β-cyclodextrin, was evaluated using nuclear magnetic resonance and phase solubility studies. The complex, in solid state, was prepared through kneading and physical mixture and then characterized by Fourier transform infrared spectroscopy, differential scanning calorimetry and scanning electron microscopy. By means of confocal laser scanning microscopy, the effect of proline on the morphology of *Candida albicans* was evaluated. Microbiological assays were performed to evaluate the antifungal activity of the complex against *C. albicans*. The results obtained from phase solubility assays showed that the complexation of ketoconazole is an effective strategy to enhance its solubility. Confocal laser scanning microscopy demonstrated that proline severely affected *Candida* morphology, and microbiological studies established high antifungal activity for the complex, signifying an advantage, and therefore, a potential improvement in its application areas.

Keywords: ketoconazole, multicomponent complex, solubility, antifungal activity.

Chemical compounds studied in this article: Ketoconazole (PubChem CID: 47576), 46 β -cyclodextrin (PubChem CID: 444041), L-Proline (PubChem CID: 145742).

1. INTRODUCTION

Recently, an increase in the prevalence and incidence of invasive fungal infections has been reported, with *Candida* as one of the most common genera causing infections [1]. *Candida* is an opportunistic type of yeast that causes severe disease in immunocompromised individuals. For example, oropharyngeal candidiasis is a frequent infection of individuals undergoing immunosuppressive therapy for cancer, organ transplantation and in AIDS patients [2,3]. The common treatment of candidiasis is associated with several side effects that limit the dose and dosing frequency. Therefore, new drugs and drug formulations that permit the reduction in dose and mitigation of side effects are urgently required for the efficient management of *Candida* infections [4].

Ketoconazole (KET, Fig. 1A), a dibasic imidazole synthetic agent with a broad spectrum of antifungal activity, is used to treat mycotic infections, including candidiasis [5]. KET is classified as a class II drug in the Biopharmaceutics Classification System, because of its low solubility and high permeability. Its' limited water solubility generates problems in the preparation of pharmaceutical formulations and limits its bioavailability and therapeutic applications.

Many technologies that improve the solubility of drugs that are poorly water-soluble have been developed, such as the incorporation of cyclodextrins (CDs) [6]. CDs are, in fact, water soluble cyclic oligosaccharides composed of 6 (α-CD), 7 (β-CD, Figure 1B) or 8 (γ-CD) D-(+)-glucopyranose units, arranged in a truncated cone shaped structure. Different molecules can penetrate into the relatively hydrophobic cavity and form non covalent inclusion complexes, thus modifying their physical, chemical and biological properties [7-11]. In previous work, the preparation and characterization of KET complexes with CDs were reported. The researchers demonstrated that these inclusion complexes were an effective way to increase the solubility of KET [12-15]. In addition, in recent years the use of

multicomponent complexes with CDs and a third auxiliary substance has become more popular, in order to facilitate the therapeutic application of different drugs [6, 16-20]. With regard to KET, multicomponent complexes were prepared with acids compounds as the third compound and compared to a binary system demonstrating the multicomponent systems a better pharmaceutical performance [13, 21, 22]. Amino acids are widely used in chemical, microbiological and pharmaceutical fields, and their incorporation into CD complexes has been reported to be an effective technology for enhancing the solubility and bioavailability of compounds with poor water solubility [23]. We have previously reported that glycine and cysteine increase chloramphenicol solubility by formation of a multicomponent complex with β-CD that modulates reactive oxygen species production induced by this drug in leukocytes [24].

The aim of this study was to investigate the influence of the complexation of KET with β-CD and L-Proline (PRO) (Fig. 1C) on its solubility in aqueous solutions and antifungal activity. PRO was selected because it induces germ tube-forming cells in *C. albicans* cultures, which are more sensitive to azole-induced killing than the yeast cell itself, whereby a synergistic effect between KET and PRO could be observed [25]. Phase solubility analyses and nuclear magnetic resonance spectroscopy were used to determine the effects of complexation on drug solubility and affinity constant. The complexes, in solid state, were prepared by the kneading and physical mixture methods and then characterized by Fourier transform infrared spectroscopy, scanning electron microscopy and thermal analysis. A microbiological *in vitro* assay of KET and the KET:β-CD:PRO multicomponent complex was performed using *C. albicans,* an important clinical pathogen. The inhibition zone diameter, in each case, was measured, and the obtained value served as a measure of the antifungal activity of KET. In addition, confocal laser scanning microscopy (CLSM) was used to evaluate the effect of PRO on *C. albicans* morphology.

2. MATERIALS AND METHODS

2.1. Chemicals and reagents

KET and PRO were obtained from Todo Droga (Argentina). β-CD (MW = 1135) was kindly supplied by Roquette (France). Dimethyl sulfoxide-D_6 (99.8 %) MagniSolv™ deuterated solvent was obtained from Merck (Switzerland). All other materials and solvents were of analytical reagent grade. A Milli-Q Water Purification System (Millipore, USA) generated the water used in these studies.

2.2. Phase solubility analysis

Experiments were carried out in stoppered glass tubes containing an excess amount of KET (15 mg) and 5 ml of increasing concentrations of β-CD (0–13.2 mM) in the presence of PRO (10 mM), according to the method reported by Higuchi and Connors [26]. The tubes were placed in a 37.0 (±0.1) ºC thermostatized shaker (Ferca) for 72 h at 130 rpm, until complexation equilibrium was reached. Each sample suspension was filtered through a 0.45 µm membrane (Millipore), and the concentration of KET in the filtered solutions was measured by UV spectrophotometry at 225 nm (Agilent Cary 50 spectrophotometer). Each experiment was repeated at least three times, and the results reported were the mean values. The K_c value for the corresponding KET complex was calculated from the slope of the phase-solubility diagrams and intrinsic solubility (S_0) according to Eq. (1):

$$K_c = \text{slope} / S_0 (1 - \text{slope}) \qquad \text{Eq. (1)}$$

2.3. NMR studies

The NMR spectra of pure compounds and the multicomponent system were recorded on a Bruker Avance II high resolution spectrometer equipped with a broad band inverse probe (BBI) and a variable temperature unit (VTU). The spectra were measured at 298 K. DMSO

125 deuteration degree min 99.8% was used as solvent. Induced changes in the ^{1}H chemical shifts
126 for KET, β-CD and PRO, which originated due to their complexation, were calculated using
127 the following equation Eq. (2):

128 $$\Delta\delta = \delta_{complex} - \delta_{free} \qquad \text{Eq. (2)}$$

129

130 **2.4. Preparation of complexes in solid state**

131 The solid complexes of KET with β-CD and PRO, in a 1:1:1 molar ratio, were prepared using
132 the kneading (K) and physical mixture (PM) methods:
133 a) Kneading: KET, β-CD, and PRO powders, in a 1:1:1 molar ratio, were mixed and then
134 crushed with a mortar and pestle, adding a water:ethanol solution (1:1 v/v). The mix was
135 kneaded for 30 min and then dried at 45 °C for 24 h.
136 b) Physical mixture: was prepared by uniformly mixing KET with β-CD and PRO powders in
137 a mortar in a 1:1:1 molar ratio.

138

139 **2.5. Fourier transform infrared spectroscopy (FTIR)**

140 FTIR spectra of KET, β-CD, PRO and the complex (KBr disks) were recorded on a Nicolet
141 Avatar 360 FTIR spectrometer. The spectrum of the complex was compared with those of
142 pure KET, β-CD, PRO and the corresponding physical mixture. All spectra were obtained and
143 processed using EZ OMNIC E.S.P v.5.1 software.

144

145 **2.6. Differential Scanning Calorimetry (DSC) and Thermogravimetry (TG)**

146 The thermogravimetry (TG) test of sample was recorded on a TG Discovery series instrument
147 (TA, USA), and the differential scanning calorimeter (DSC) test was recorded on a DSC
148 Discovery series instrument (TA, USA). The thermal behaviour was studied by heating 1-2

mg of the samples in perforated aluminium capsules in a nitrogen atmosphere, in the temperature range of 25-200°C (DSC) and 25-350°C (TG) at a heating rate of 10°C min^{-1}.

2.7. Scanning electron microscopy studies (SEM)

Microscopic morphological structures of the solid samples were investigated and photographed using a Carl Zeiss Σigma scanning electron microscope, at the Laboratorio de Microscopía y Análisis por Rayos X (LAMARX) of the National University of Córdoba. The samples were fixed on a brass stub using double-sided aluminium tape, and to improve the conductivity, they were gold/palladium-coated under vacuum, employing a sputter coater Quorum 150. The magnification selected was sufficient to appreciate, in detail, the general morphology of the samples under study.

2.8. Analysis of cell morphology of *Candida albicans* using confocal laser scanning microscopy (CLSM)

To evaluate the effect of PRO on cell morphology, two clinical isolates of *C. albicans* (strains 216 and 256, identified by a battery of biochemical tests) were grown on 2% Sabouraud agar (24 h at 37 °C), with and without PRO (at two concentrations 10 or 100 mM). A drop of the suspended culture was transferred on a slide, fixed and stained with safranin. The samples were examined by confocal laser scanning microscopy (Olympus OLS4100) with a sufficient magnification to appreciate, in detail, the morphology of the *C. albicans* cells.

2.9. Microbiological assay

Antimicrobial susceptibility tests were performed by the agar diffusion method according to Marzouk et al., [15] with some modifications. Microorganisms and inoculum cultures of *C. albicans* were cultivated on 2% Sabouraud agar and maintained in test tubes in a refrigerator

at 4 ± 2 °C until use. The microorganisms were suspended in 0.9 % NaCl; the concentration of the obtained suspension was adjusted to 0.08-0.1 of absorbance at 600 nm, using a spectrophotometer analyser (~10^7 colony forming units per millilitres, Shimadzu UV-Mini 1240 spectrophotometer). The surface of the agar plates was spread using a sterile swab soaked in the bacterial suspension. A 6-mm disk of sterile Whatman N°1 membrane filter resting on an agar culture medium was inoculated with 5 µl of solution containing free or complexed KET (7 µg) and KET:PRO. Aqueous solutions of pure β-CD and PRO were used as controls. The plates were incubated at 37 °C for 24 h. The resulting zone diameters of growth inhibition were then measured in mm. Each determination was performed in triplicate, statistics values were expressed as the mean ± the standard deviation of each group. The difference between three means was compared by a two-tailed unpaired Student's t test. P values of < 0.05 were considered significant.

3. RESULTS AND DISCUSSION

3.1. Behaviour of the multicomponent complex in aqueous solution

3.1.1. Phase solubility analysis (PSA)

In order to determine the influence of β-CD and PRO on KET solubility, the phase-solubility diagram was determined. The phase solubility profile of KET with β-CD and PRO can be classified as A_L type, according to Higuchi and Connors. [26] These profiles showed a linear increase of drug solubility (data not shown), when the concentration of β-CD increased, which is indicative of the formation of soluble complexes. The corresponding stability constant value, calculated from phase-solubility diagram, was 4966 ± 93 M^{-1}, and the increases in drug solubility were of 65-fold (S_0 0.0094 mg/ml and S_{max} 0.609 mg/ml).

3.1.2. NMR studies

NMR studies were performed to confirm the inclusion complex formation and to gain insight into the structure of the multicomponent complex. In Table 1, the assignments of the KET, β-CD and PRO peaks and the chemical shift displacement (Δδ) due to complexation (for NMR signal notation see Fig. 1) are shown. The changes observed in NMR signals clearly indicated the compound interactions (Fig. 2). In the case of β-CD, the inner protons (H_3 and H_5) undergo an upfield shift that can be attributed to magnetic anisotropy effects caused by the KET inclusion. Furthermore, OH_2 and OH_3 protons of β-CD showed a marked shielding effect that suggested that some moiety of KET and/or PRO molecules can interact with the macromolecule's wide rim, possibly establishing hydrogen bond interactions. In addition, the protons of the dichlorophenyl (H_{24} and H_{26}) and phenolic ($H_{10\text{-}14}$ and $H_{11\text{-}13}$) rings of KER exhibited significant upfield shifts, indicating its penetration inside the β-CD cavity. These observations are consistent with the existence of two different inclusion modes for the complex. The downfield observed for the KET imidazole ring (H_{30}, H_{31} and H_{33}) and PRO (H_β, H_γ and H_δ) protons, may be due to conformational changes produced by the interaction between compounds.

3.2. Behaviour of the multicomponent complex in solid state

3.2.1. Fourier transform infrared spectroscopy (FTIR)

In order to confirm whether KET could interact with PRO and β-CD, IR spectrum analysis of pure compounds, and systems prepared by kneading and physical mixture, were developed. As shown in Fig. 3A, the IR spectrum of pure KET was characterized by absorption peaks at 1645 cm^{-1} (C-O stretching vibration), 1583 cm^{-1} (aromatic C-C stretching vibration) and 1512 and 1457 cm^{-1} (benzene cycle vibration). The IR spectrum of β-CD (Fig. 3B) showed prominent absorption bands at 3365 cm^{-1}, (O-H stretching vibration) while strong bands of pure PRO (Fig. 2C) appeared at 1619 cm^{-1} (asymmetric COO^- stretching vibration) and 1401

224 cm^{-1} (symmetric COO^- stretching vibration). The spectra of multicomponent systems
225 prepared by PM (Fig. 3D) or K (Fig. 3E) did not show any new peaks, indicating no chemical
226 bond formation in these systems. The IR spectrum of the PM system did not significantly
227 differ from those of the single components, indicating that there is almost no interaction
228 between these compounds when physically mixed. On the other hand, in the IR spectrum of
229 the system prepared by K, a widening and a marked shift of the characteristic absorption
230 bands of KET was observed, compared with the pure drug. It was possible to observe that the
231 bands of PRO are almost masked by the very intense and broad β-CD and KET bands
232 although can be observed the modification that appear at 1619 cm^{-1} in pure PRO. These
233 findings indicated the presence of interactions between the KET, β-CD and PRO in this
234 system.

235 **3.2.2. Differential Scanning Calorimetry (DSC) and Thermogravimetry (TG)**

236 The DSC and TG curves of pure components and multicomponent systems are shown in Fig.
237 4. It can be observed that KET presents a sharp endothermic peak at 149.8 °C, attributable to
238 the melting process of the crystalline form of the drug, which begins to decompose at about
239 320 °C. PRO and βCD lost water at temperatures between 25–100 °C (Δm= 5% and 7.5%,
240 respectively), with decomposition taking place above 200 °C (PRO) and 300 °C (β-CD), as
241 evidenced by the mass loss observed in the TG curve. TG curves of KET:β-CD:PRO PM and
242 K systems show a similar behaviour with three steps of weight loss, one due to dehydration
243 (Δm= 7.1% PM and 4.6 % K), a second event related to PRO decomposition (Δm= 7% PM
244 and K) and the third corresponding to the drug and β-CD decomposition taking place above
245 300°C. In the DSC curve KET:β-CD:PRO PM, it is possible to observe the endothermic event
246 corresponding to the melting point of the drug at 148.2 °C. On the other hand, the thermal
247 peak of the drug in the KET:β-CD:PRO K curve, appeared at a lower temperature (142.2 °C),

accompanied by a reduction in its fusion enthalpy, suggesting that a partial drug amorphization occurred in this system that can be related to the complexation.

3.2.3. Scanning electron microscopy (SEM)

The shape and structure of KET complexes prepared by the K method were assessed by SEM (Fig. 5), and were compared with the pure materials and KET systems prepared by PM. In SEM images of KET:β-CD:PRO K, it was observed that these products had a significantly different morphology, with respect to the pure materials and the PM, and it was not possible to differentiate the single components. These solids showed small size particles, compared with the pure compounds. On the other hand, the characteristic KET crystals, which were mixed with β-CD particles and PRO, were clearly detectable in the SEM images of the PM, thus confirming the presence of the crystalline drug and the absence of interactions.

3.3. Confocal laser scanning microscopy (CLSM) observation

The effect of PRO on *C. albicans* morphology was evaluated by CLSM after the incubation of the yeast strains with PRO at two concentrations (10 and 100 mM). The alteration on cellular morphology was visually confirmed by CLSM, which showed a unicellular, oval-shaped diploid fungus in both strains when not treated with PRO (control, Fig. 6. a and d). The dose-dependent interference of PRO with the morphology of *C. albicans* could be clearly seen in strain 216. In the case of treatment with PRO 10 mM (Fig. 6 b), it was possible to observe some cells with altered morphology, while for the treatment with PRO 100 mM (Fig. 6 c), a cell pattern with totally altered morphology was evident. In strain 256, only 100 mM of PRO altered its morphology (Fig. 6 f). This microscopic observation confirms the ability of PRO to induce germ tube formation and morphological changes in *C. albicans*. [25]

3.4. Microbiological assay

The antifungal activity of KET, β-CD, PRO, PRO:β-CD, KET:PRO, KET:β-CD and KET:β-CD:PRO was studied in *C. albicans* 216 and 256 clinical pathogen isolates. The diffusion agar method was used for this study. β-CD and PRO used as negative control did not show inhibition halos (data not shown). In Fig. 7, we can observe the microbiological data from KET, KET:PRO, KET:β-CD and the KET:β-CD:PRO complex. β-CD, PRO, PRO:β-CD.

β-CD, PRO and PRO: β-CD were used as control and did not present inhibition halo.

The antifungal activity of the KET:β-CD:PRO multicomponent complex was significantly higher than KET and that of KET:β-CD and KET:PRO, suggesting a synergistic effect between PRO and KET, solubilized by the presence of β-CD. It is known that the formation of inclusion complexes is able to increase, decrease or maintain the biological activity, depending on the balance between microscopic or macroscopic effects. Indeed, on the microscopic scale, inclusion leads to the reduction of free drug, whereas on the macroscopic scale, complexation of slightly soluble drug considerably improves its water solubility, which can increase the available drug concentration. In this work despite the high Kc value obtain for the complex (4966 ± 93 M^{-1}), the microbiological activity was increased assessing the ability of β-CD to release the drug. Moreover, it was suggested that CD molecules might destabilize the outer membrane of the microorganisms, which eventually leads to an increase of the diffusion rate of antimicrobials [27]. Furthermore, this synergy may be attributable to the presence of PRO that altered the *C. albicans* morphology, as could be observed by CLSM. This increase in the antifungal activity of the KET:β-CD:PRO multicomponent complex is the most favourable aspect of the development system.

4. Conclusions

In this work, the KET:β-CD:PRO multicomponent complexes were prepared in solution and solid state and characterized by PSA, NMR, FTIR, SEM and DSC studies. The results obtained showed that the formation of a multicomponent complex of KET with β-CD and PRO produces an important increase in the aqueous solubility of this antifungal drug. Moreover, PRO induces alterations in the cellular morphology of *C. albicans*. It can be suggesting that the synergy of both effects results in the highest antifungal activity observed for the KET:β-CD:PRO complex. Thus, this multicomponent complex is an interesting candidate for the preparation of KET dosage forms, with improved antifungal activity.

ACKNOWLEDGMENTS

The authors wish to acknowledge the assistance of the Consejo Nacional de Investigaciones Científicas y Técnicas (CONICET), the Universidad Nacional de Córdoba, Fondo para la Investigación Científica y Tecnológica (FONCYT) Préstamo BID PICT 2013-2150, and the Secretaría de Ciencia y Técnica de la Universidad Nacional de Córdoba (SECyT) which provided support and facilities for this investigation. We also thank Ferromet S.A. (agent of Roquette in Argentina) for its donation of β-cyclodextrin. We are grateful to Dr. Gloria Bonetto for NMR measurements and for her helpful discussions on the ^{1}H NMR spectra.

322 **References**

323 [1] R. Fernández-García, E. de Pablo, M.P. Ballesteros, D.R. Serrano, Unmet clinical needs in
324 the treatment of systemic fungal infections: The role of amphotericin B and drug targeting.
325 Int. J. Pharm. 1 (2017)139–148.

326 [2] K. Trautwein-Weidner, A. Gladiator, S. Nur, P. Diethelm, S. Leibund Gut-Landmann, IL-
327 17-mediated antifungal defense in the oral mucosa is independent of neutrophils. Mucosal
328 Immunol. 8 (2015) 221–31.

329 [3] G. Weindl, J.R. Naglik, S. Kaesler, T. Biedermann, B. Hube, H.C. Korting, M. Schaller,
330 Human epithelial cells establish direct antifungal defense through TLR4-mediated signaling.
331 J. Clin. Invest. 117 (2007) 3664–72.

332 [4] B. Sawant, Khan T, Recent advances in delivery of antifungal agents for therapeutic
333 management of candidiasis. Biomed. Pharmacother. 96 (2017) 1478–1490.

334 [5] J.W. Lubach, J.Z. Chen, J. Hau, J. Imperio, M. Coraggio, L. Liu, H. Wong, Investigation
335 of the rat model for preclinical evaluation of pH-dependent oral absorption in humans. Mol.
336 Pharm. 10 (2013) 3997–4004.

337 [6] T. Taupitz, J.B. Dressman, S. Klein, In vitro tools for evaluating novel dosage forms of
338 poorly soluble, weakly basic drugs: case example ketoconazole. J. Pharm. Sci. 102 (2013)
339 3645–52.

340 [7] V. Aiassa, A. Zoppi, M.C. Becerra, I. Albesa, M.R. Longhi, Enhanced inhibition of
341 bacterial biofilm formation and reduced leukocyte toxicity by chloramphenicol-βcyclodextrin-
342 Nacetylcysteine complex. Carbohydr. Polym. 5 (2016) 672–8.

[8] T. Loftsson, M.E. Brewster, Pharmaceutical applications of cyclodextrins: Basic science and product development. J. Pharm. Pharmacol. 62 (2010) 1607–21.

[9] T. Loftsson, M.E. Brewster, Cyclodextrins as functional excipients: methods to enhance complexation efficiency. J. Pharm. Sci. 101 (2012) 3019–32.

[10] J.Q. Zhang, K.M. Jiang, K. An, S.H. Ren , X.G. Xie , Y. Jin , J. Lin, Novel wáter soluble fisetin/cyclodextrins inclusion complexes: Preparation, characterization, molecular docking and bioavailability. Carbohydr. Res. 11 (2015) 20–8.

[11] A. Zoppi, A. Delrivo, V. Aiassa, M.R. Longhi. Binding of sulfamethazine to β-cyclodextrin and methyl-β-cyclodextrin. AAPS Pharm. Sci. Tech. 14 (2013) 727–35.

[12] M. Demirel, G. Yurtdas, L. Genc, Inclusion complexes of ketoconazole with beta-cyclodextrin: physicochemical characterization and in vitro dissolution behaviour of its vaginal suppositories. J. Incl. Phenom. Macrocycl. Chem. 70 (2011) 437–445.

[13] M.T. Esclusa-Díaz, M. Guimaraens-Méndez, M.B. Pérez-Marcos, J.L. Vila-Jato, J.J.Torres-Labandeira, Characterization and in vitro dissolution behavior of ketoconazole/β- and 2-hydroxypropyl-β-cyclodextrin inclusion compounds. Int. J. Pharm. 143 (1996a) 203–10.

[14] M.T. Esclusa-Díaz, M. Gayo-Otero, M.B. Pérez-Marcos, J.L. Vila-Jato, J.J. Torres-Labandeira, Preparation and evaluation of ketoconazole-β-cyclodextrin multicomponentcomplexes. Int. J. Pharm. 142 (1996b) 183–87.

[15] M.A. Marzouk, A.A. Kassem, A.M. 304 Samy, R.I. Amer. Comparative evaluation of ketoconazole-β-cyclodextrin systems prepared by coprecipitation and kneading, Drug Discov. Ther. 4 (2010) 380–7.

[16] R. Chadha, M. Bala, P. Arora, D.V.S. Jain, R.R.S. Pissurlenkar, E.C. Coutinho, Valsartan inclusion by methyl-β-cyclodextrin: Thermodynamics, molecular modelling, Tween 80 effect and evaluation. Carbohydr. Polym.103 (2014) 300–9.

[17] P.N. De Melo, E.G. Barbosa, L.B. De Caland, H. Carpegianni, C. Garnero, M. Longhi, M. De Freitas Fernades-Pedrosa, A.A. Da Silva-Júnior, Host-guest interactions between benznidazole and beta-cyclodextrin in multicomponent complex systems involving hydrophilic polymers and triethanolamine in aqueous solution. J. Mol. Liq. 186 (2013) 147–56.

[18] C. Garnero, M.R. Longhi, Study of ascorbic acid interaction with hydroxypropyl-beta-cyclodextrin and triethanolamine, separately and in combination. J. Pharm. Biomed. Anal. 45 (2007) 536–545.

[19] Garnero, M. Longhi, Development of HPLC and UV spectrophotometric methods for the determination of ascorbic acid using hydroxypropyl-β-cyclodextrin and triethanolamine as photostabilizing agents. Anal. Chim. Acta. 659 (2010) 159–66.

[20] M.J. Mora, M.R. Longhi, G.E. Granero, Synthesis and characterization of binary and ternary complexes of diclofenac with a methyl-β-CD and monoethanolamine and in vitro transdermal evaluation. Eur. J. Med. Chem. 45 (2010) 4079–88.

[21] A. Gerlóczy, J. Szemán, K. Csabai, I. Kolbe, L. Jicsinzky, D. Acerbi, P. Ventura, E. Redenti, J. Szejtli. Pharmacokinetic study of orally administered ketoconazole and its multicomponent complex on rabbits of normal and low gastric acidity. In: Szejtli J, Szente L, eds. *Proceedings of the eighth international symposium on cyclodextrins*, Dordrecht: Kluwer Academic Publishers; (1996) 515–518.

[22] A. Selva, E. Redenti, P. Ventura, M. Zanol, B. Casetta, Study of β-cyclodextrin–ketoconazole–tartaric acid multicomponent non-covalent association by positive and negative ionspray mass spectrometry. J. Mass Spectrom. 33 (1998) 729–734.

[23] P. Mura, F. Maestrelli, M. Cirri, Ternary 327 systems of naproxen with hydroxypropyl beta-cyclodextrin and aminoacids. Int. J. Pharm. 260 (2003) 293–302.

[24] V. Aiassa, A. Zoppi, I. Albesa, M.R. Longhi, Inclusion complexes of chloramphenicol with β-cyclodextrin and aminoacids as a way to increase drug solubility and modulate ROS production. Carbohydr. Polym.121 (2015) 320–7.

[25] M. Niimi, A. Kamiyama, M. Tokunaga, J. Tokunaga, H. Nakayama, Germ tube-forming cells of *Candida albicans* are more susceptible to clotrimazole-induced killing than yeast cells. Sabouraudia. 23 (1985) 63–68.

[26] T. Higuchi, K.A. Connors, Phase-solubility techniques. Adv. Anal. Chem. Instrum. 4 (1965) 117–212.

[27] V. Nardello-Rataj, L. Leclercq, Encapsulation of biocides by cyclodextrins: toward synergistic effects against pathogens, Beilstein J. Org. Chem. 10 (2014) 2603–2622.

Figure legends

Figure 1: Chemical structure and proton atom assignment scheme of: (A) KET, (B) β-CD, (C) PRO.

Figure 2. ^{1}H NMR Spectra of (A) KET, (B) βCD, (C) PRO and (D) KET:βCD:PRO system.

Figure 3. IR spectra of: a) KET, b) β-CD, c) PRO, d) KET:β-CD:PRO K, e) KET:β-CD:PRO PM.

Figure 4. DSC and TG curves of KET (fuchsia), β-CD (green), PRO (black), KET:βCD:PRO K system (blue) and KET:βCD:PRO PM system (turquoise).

Figure 5. Scanning electron microphotographs of: (a) KET, (b) β-CD, (c) PRO, (d) KET:βCD:PRO K (e) KET:βCD:PRO PM.

Figure 5. Confocal laser scanning microscopy of: (a) strain 216 control, (b) strain 216 with PRO 10 mM, (c) strain 216 with PRO 100 mM, (d) strain 256 control (e) strain 256 with PRO 10 mM and f) strain 256 with PRO 100 mM.

Figure 7: Histogram of the mean values of the inhibition zones diameters of KET, KET:PRO, KET:β-CD and KET:β-CD:PRO. White column, *Candida albicans* 256; black column, *C. albicans* 216. *$p < 0.05$ with respect to KET, $^{\#}$ $p < 0.05$ compared to KET:PRO, ~ $p < 0.05$ compared to KET:β-CD

Highlights

- KET complex with β-cyclodextrin and Proline was prepared and characterized
- The water solubility of KET was improved
- The antifungal activity was increase by multicomponent complex formation
- The multicomponent complex results a good candidate to optimize KET formulations

A)

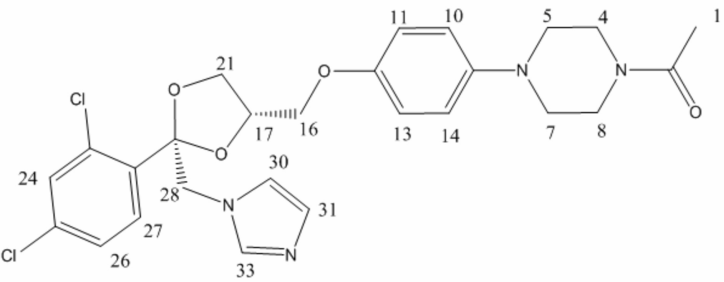
Cl
Cl
O
O
O
O
N
N
N
N
O
1
4
5
7
8
10
11
13
14
16
17
21
24
26
27
28
30
31
33

B)

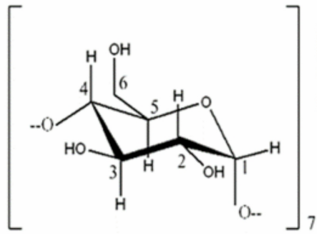
H
OH
6
4
5
H
O
--O
HO
3
H
2
OH
1
H
H
O--
7

C)

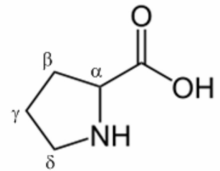
O
OH
β
α
γ
NH
δ

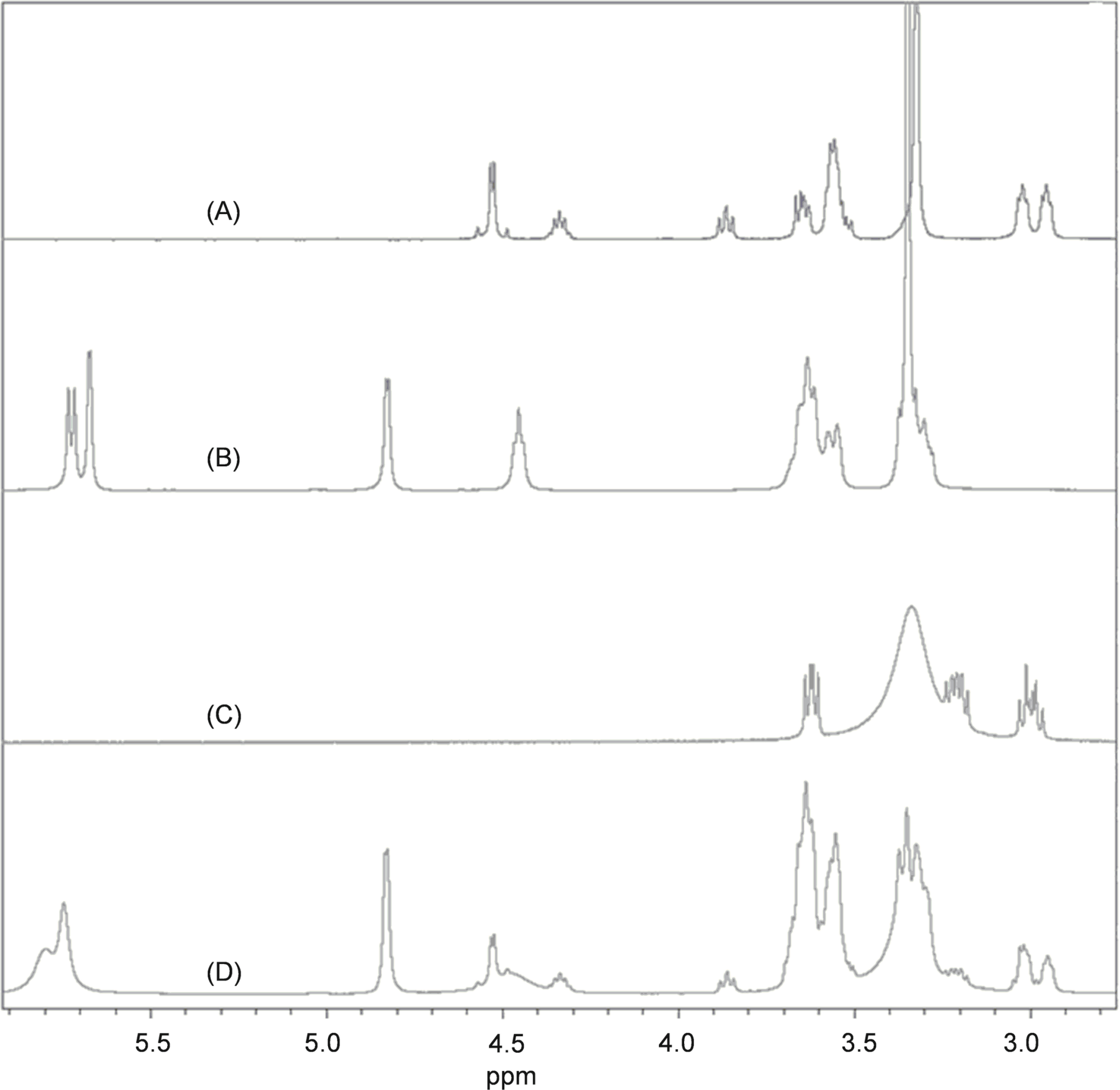
(A)
(B)
(C)
(D)
5.5
5.0
4.5
4.0
3.5
3.0
ppm

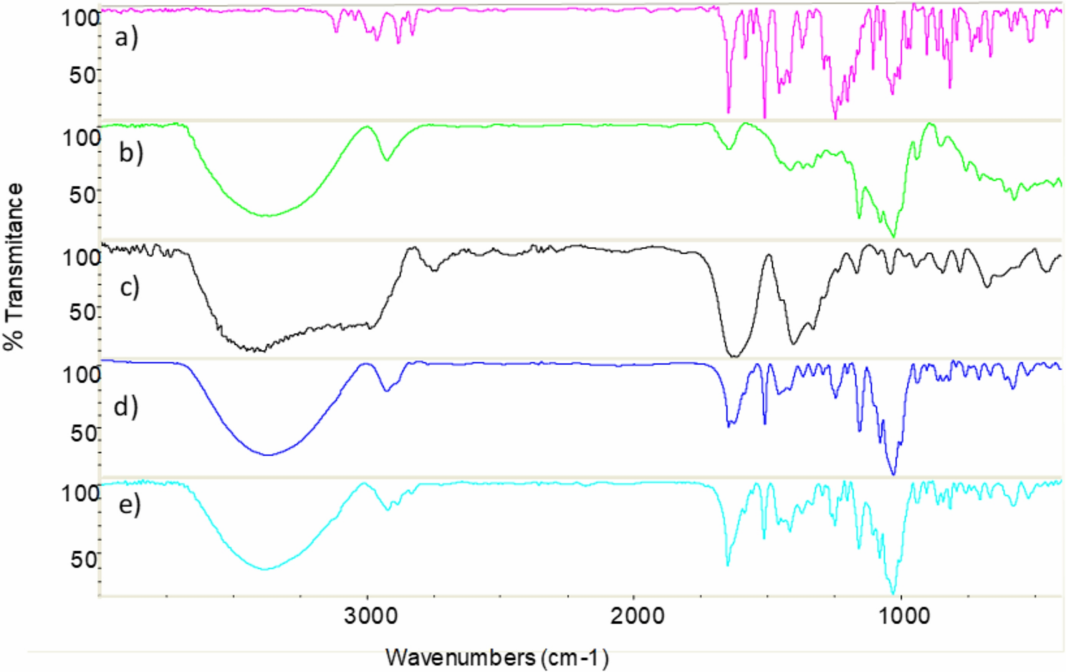
100
50
a)
b)
c)
d)
e)
% Transmitance
3000
2000
1000
Wavenumbers (cm-1)

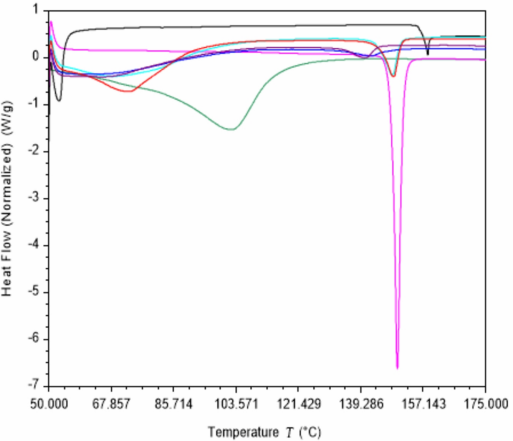
Heat Flow (Normalized) (W/g)
1
0
-1
-2
-3
-4
-5
-6
-7
50.000
67.857
85.714
103.571
121.429
139.286
157.143
175.000
Temperature T (°C)

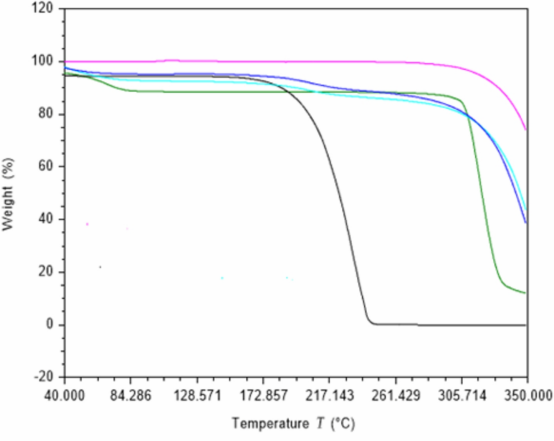
Weight (%)
120
100
80
60
40
20
0
-20
40.000
84.286
128.571
172.857
217.143
261.429
305.714
350.000
Temperature T (°C)

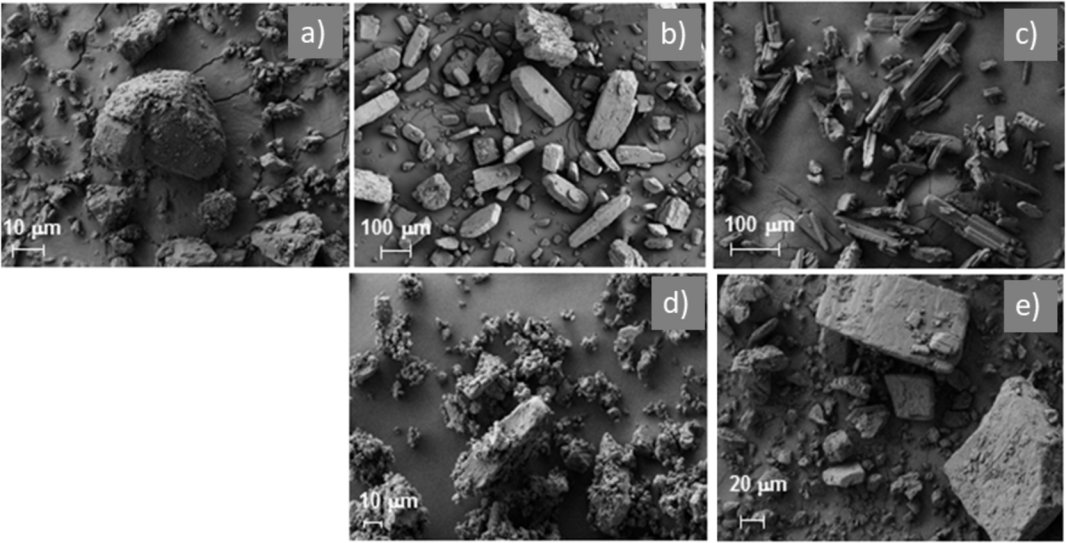
a)
10 µm
b)
100 µm
c)
100 µm
d)
10 µm
e)
20 µm

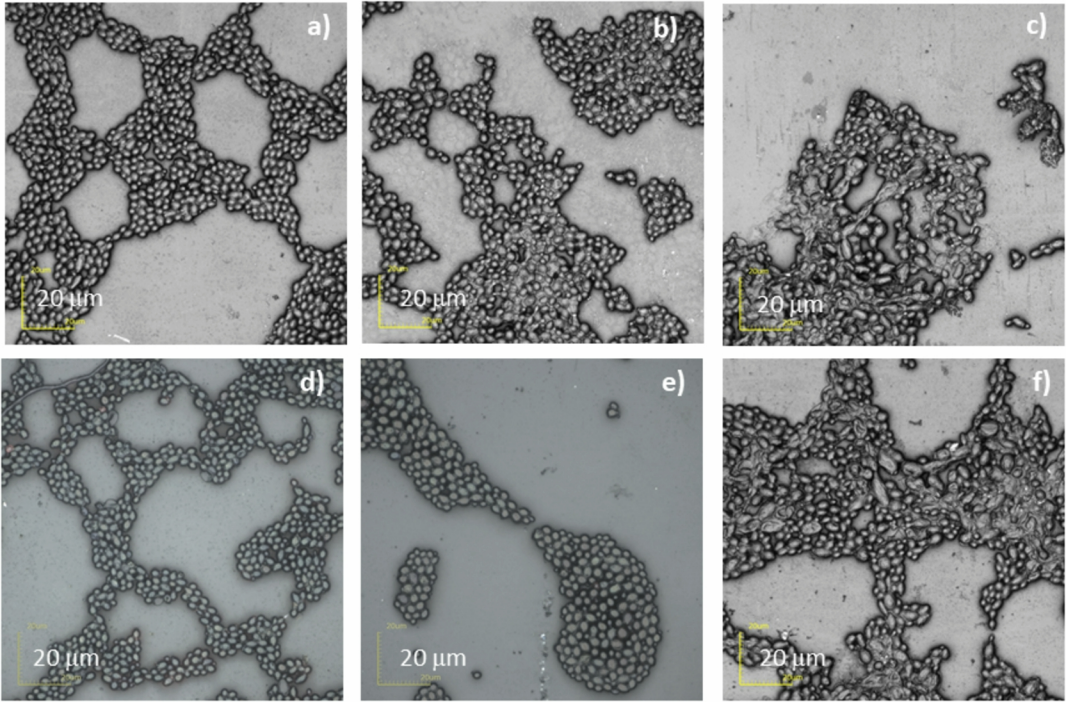
a)
20 µm
b)
20 µm
c)
20 µm
d)
20 µm
e)
20 µm
f)
20 µm

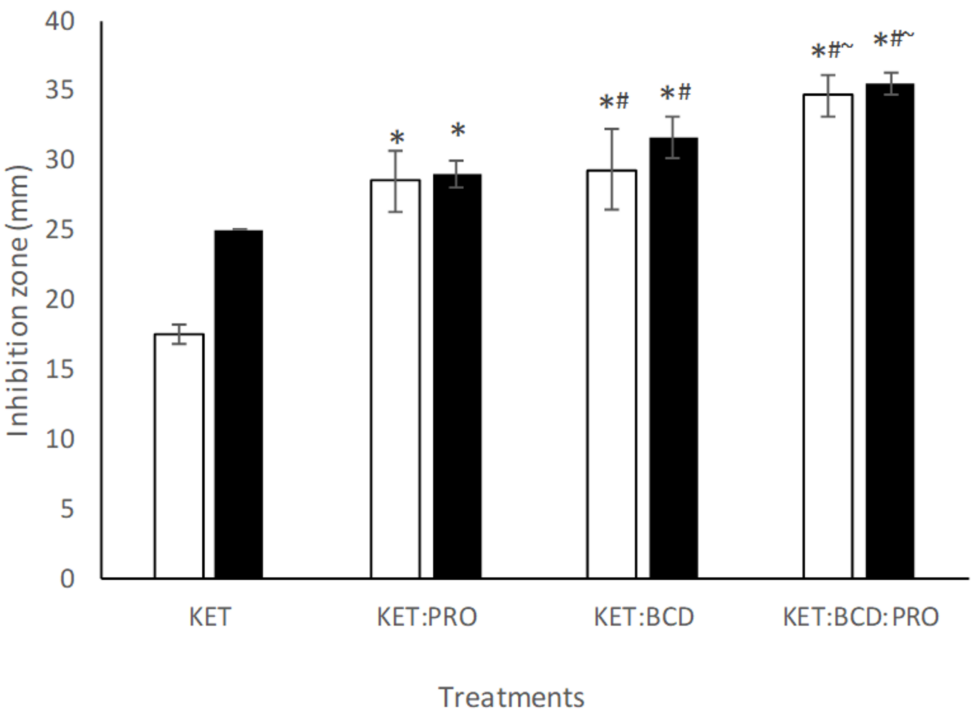
40
35
30
25
20
15
10
5
0
Inhibition zone (mm)
*
*
*#
*#
*#~
*#~
KET
KET:PRO
KET:BCD
KET:BCD:PRO
Treatments

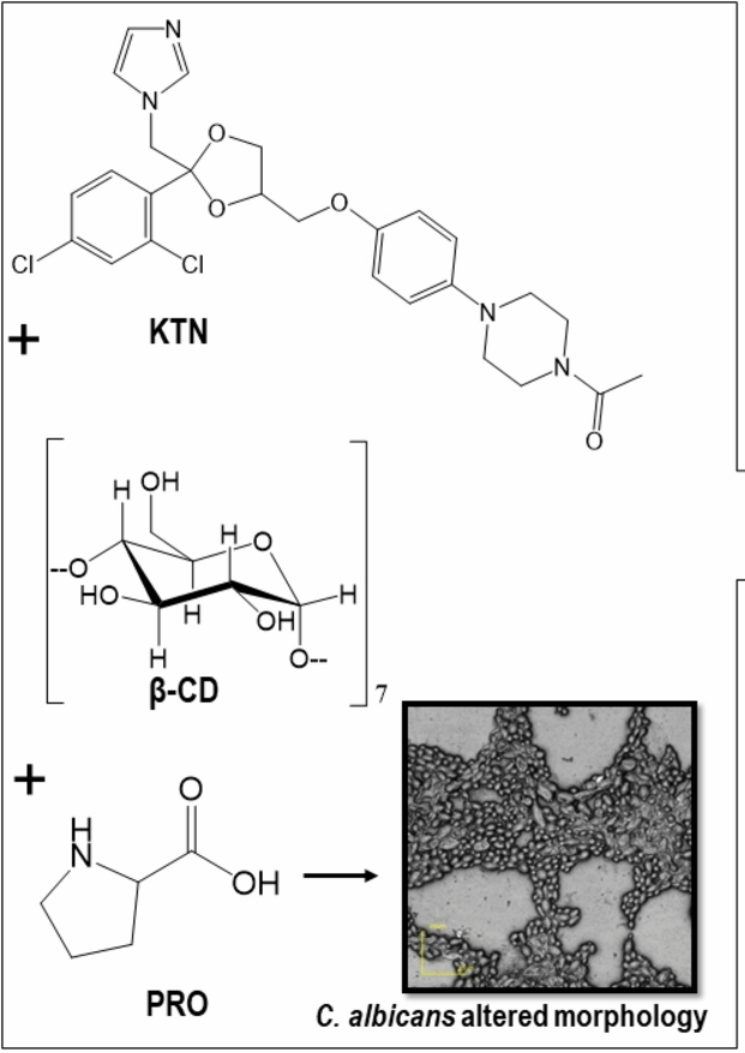

Kneading
EtOH:H_2O

Increase water solubility
K_c= 4966 ± 93 M^{-1}

KTN:β-CD:PRO multicomponent complex

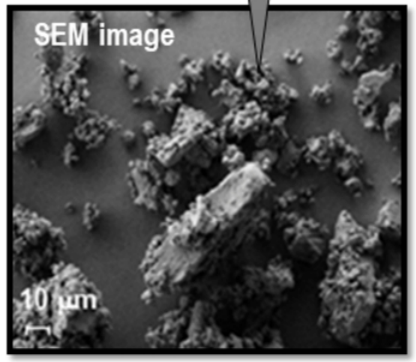

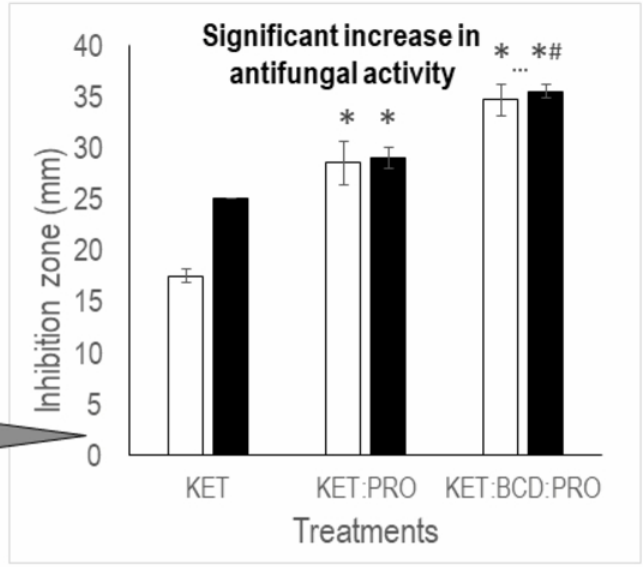

Table 1: Chemical shifts for the protons of KET, β-CD and PRO in the free and complex form.

KET protons	**δ (ppm)**	**δ (ppm) KET:β-CD:PRO**	**Δδ (ppm)**
H_1	2.0312	2.0298	-0.0014
H_{4-8}	-	overlapped	-
H_{5-7}	-	overlapped	-
H_{16}	-	overlapped	-
H_{21}	-	overlapped	-
H_{17}	4.3359	4.3359	0
H_{28}	4.5262	4.5253	-0.0009
H_{11-13}	6.7956	6.7926	-0.0003
H_{31}	6.8136	6.8140	0.0004
H_{10-14}	6.9113	6.9086	-0.0027
H_{30}	7.0083	7.0093	0.0010
H_{26}	7.4523	7.4509	-0.0014
H_{33}	7.4728	7.4779	0.0051
H_{27}	7.5657	7.5657	0
H_{24}	7.6837	7.6811	-0.0026
β-CD protons			
H_1	4.8241	4.8276	0.0035
H_2	-	overlapped	-
OH_2	5.7216	5.7943	0.0727
H_3	3.6284	3.6347	-0.0063
OH_3	5.6699	5.7437	0.0738
H_4	-	overlapped	-
H_5	3.5576	3.5569	-0.0007
H_6	3.6284	3.6347	-0.0063
OH_6	-	overlapped	-
PRO protons			
Hα	-	overlapped	-
Hβ	1.9691	1.9834	0.0143
Hγ	1.7205	1.7427	0.0222
Hδ	-	overlapped	-
	3.2057	3.2078	0.0021